Cholesterol Sensitivity and Lipid Raft Targeting of Kir2.1 Channels

Victor G. Romanenko,* Yun Fang,* Fitzroy Byfield,* Alexander J. Travis,† Carol A. Vandenberg,‡ George H. Rothblat,¶ and Irena Levitan*

*Institute for Medicine and Engineering, Department of Pathology and Laboratory Medicine, University of Pennsylvania, Philadelphia, Pennsylvania; †Baker Institute for Animal Health, College of Veterinary Medicine, Cornell University, Ithaca, New York; ‡Department of Molecular, Cellular, and Developmental Biology, and Neuroscience Research Institute, University of California, Santa Barbara, California; and ¶Division of Gastroenterology and Nutrition, Department of Pediatrics, The Children's Hospital of Philadelphia, Philadelphia, Pennsylvania

ABSTRACT This study investigates how changes in the level of cellular cholesterol affect inwardly rectifying K^+ channels belonging to a family of strong rectifiers (Kir2). In an earlier study we showed that an increase in cellular cholesterol suppresses endogenous K^+ current in vascular endothelial cells, presumably due to effects on underlying Kir2.1 channels. Here we show that, indeed, cholesterol increase strongly suppressed whole-cell Kir2.1 current when the channels were expressed in a null cell line. However, cholesterol level had no effect on the unitary conductance and only little effect on the open probability of the channels. Moreover, no cholesterol effect was observed either on the total level of Kir2.1 protein or on its surface expression. We suggest, therefore, that cholesterol modulates not the total number of Kir2.1 channels in the plasma membrane but rather the transition of the channels between active and silent states. Comparing the effects of cholesterol on members of the Kir2.x family shows that Kir2.1 and Kir2.2 have similar high sensitivity to cholesterol, Kir2.3 is much less sensitive, and Kir2.4 has an intermediate sensitivity. Finally, we show that Kir2.x channels partition virtually exclusively into Triton-insoluble membrane fractions indicating that the channels are targeted into cholesterol-rich lipid rafts.

INTRODUCTION

Inwardly rectifying K^+ (Kir) channels are known to play critical roles in the maintenance of the membrane potential and K^+ homeostasis, which in turn regulate the excitability of muscle cells and neurons (Hille, 1992; Lopatin and Nichols, 2001). Downregulation of the Kir current was shown to be associated with heart failure (Beuckelmann et al., 1993). Consistent with these observations, reduction of Kir2.1 current in guinea pigs by a dominant-negative Kir2.1 caused a prolonged QT interval and arrhythmia (Miake et al., 2003). Targeted disruption of Kir2.1 in mice showed that these channels are essential for K^+-induced dilation of cerebral arteries (Zaritsky et al., 2000). Furthermore, it was shown recently that mutations in Kir2.1 cause Andersen's syndrome, an autosomal dominant disorder that is characterized by cardiac arrhythmias, periodic paralysis, and dysmorphic bone structure, as well as several developmental abnormalities (Hosaka et al., 2003; Jongsma and Wilders, 2001; Lange et al., 2003; Plaster et al., 2001).

Currently, there are four known members of the Kir2 subfamily (Kir2.1–2.4). Kir2.1–2.3 channels are ubiquitously expressed in a variety of tissues, including cardiac cells (Melnyk et al., 2002; Miake et al., 2003; Wang et al., 1998; Zobel et al., 2003), vascular smooth muscle cells (Karkanis et al., 2003; Sampson et al., 2003; Zaritsky et al., 2000), and neurons (as reviewed by Neusch et al., 2003), whereas Kir2.4 expression appears to be tissue-specific (Pruss et al., 2003; Topert et al., 1998). Although strong rectification and high constitutive activity are the general biophysical properties of all Kir2.x channels, the channels differ significantly in their unitary conductances and sensitivity to Ba^{2+} block (Kubo et al., 1993; Liu et al., 2001; Makhina et al., 1994; Perier et al., 1994; Schram et al., 2003; Takahashi et al., 1994; Topert et al., 1998). There is also growing evidence that Kir2.x subunits may form functional heterotetramers with intermediate properties (Preisig-Muller et al., 2002; Schram et al., 2002, 2003; Zobel et al., 2003).

Two major factors that are known to regulate Kir2 channels are protein phosphorylation (Tong et al., 2001; Wischmeyer et al., 1998; Wischmeyer and Karschin, 1996; Zhu et al., 1999) and interaction with phosphoinositides (Huang et al., 1998; Soom et al., 2001; Zhang et al., 1999), major lipid second messengers (reviewed by McLaughlin et al., 2002, and Yin and Janmey, 2003). Our recent studies have suggested that Kir2 channels may also be regulated by the level of membrane cholesterol (Romanenko et al., 2002), a major structural component of the plasma membrane that may constitute up to 40 mol % of membrane lipids (Yeagle, 1991). Specifically, we have shown that enriching aortic endothelial cells with cholesterol significantly suppresses inwardly rectifying K^+ current, whereas cholesterol depletion enhances the current (Romanenko et al., 2002). Since endothelial Kir current has strong rectification that is a known characteristic feature of the Kir2 channels and since several

Submitted April 2, 2004, and accepted for publication September 21, 2004.

Address reprint requests to Dr. Irena Levitan, University of Pennsylvania, IME 1160 Vagelos Research Laboratories, Philadelphia, PA 19104. Tel.: 215-573-8161; Fax: 215-573-7227; E-mail: ilevitan@mail.med.upenn.edu.

Victor G. Romanenko's present address is Center for Oral Biology, Aab Institute of Biomedical Sciences, University of Rochester, Rochester, NY 14642.

0006-3495/04/12/3850/12 $2.00

doi: 10.1529/biophysj.104.043273

studies have reported that aortic endothelial cells express Kir2.1 (Eschke et al., 2002; Forsyth et al., 1997; Kamouchi et al., 1997; Yang et al., 2003), we have proposed that Kir2.1 channels are sensitive to membrane cholesterol. In this study, we test this hypothesis directly by testing cholesterol sensitivity of the Kir2.1, as well as other Kir2.x channels expressed in a null cell line that has virtually no endogenous Kir current. We show that not only Kir2.1 but all four Kir2.x channels are cholesterol-sensitive; however, they display significant differences in the degree of their cholesterol sensitivity. We also show that, consistent with the sensitivity of the channels to cholesterol, Kir2 channels partition into the Triton-insoluble membrane fractions.

MATERIALS AND METHODS

Channel expression and cell culture

Chinese hamster ovary (CHO) K1 cell line was obtained from the laboratory of Dr. Zhe Lu and maintained at 37°C in a humidified 5% CO_2 atmosphere in Ham's F-12 media (BioWhittaker, San Diego, CA) supplemented with heat-inactivated 10% fetal bovine serum (Gemini BioProducts, Woodland, CA). The cells were fed or split every 2–3 days.

Transfection protocols

Kir2.x constructs were cotransfected with enhanced green fluorescent protein (eGFP; cmv-pcDNA3.1-GFP-TOPO, Invitrogen, Carlsbad, CA) using Lipofectamine (Gibco-BRL, Gaithersburg, MD) according to the manufacturer's instructions. Kir2.1 (mouse) and Kir2.2 (mouse) clones are a gift of Dr. Kurachi, Osaka University, Japan; Kir2.4 construct (rat) is a gift from Dr. Karschin, University of Würzburg, Germany; and HA-Kir2.1 (mouse) clone, tagged with an HA epitope inserted into the extracellular M1-H5 loop (Dart and Leyland, 2001), is a gift from Dr. Caroline Dart, University of Leicester, UK. All constructs were inserted into the cmv-pcDNA3 vector.

Modulation of cellular cholesterol level

At 24 h after transfection, CHO cells were enriched with or depleted of cholesterol by incubating them with methyl-β-cyclodextrin (MβCD) saturated with cholesterol or with empty MβCD (not complexed with cholesterol), as described previously (Levitan et al., 2000). Briefly, a small volume of cholesterol stock solution in chloroform:methanol (1:1, vol/vol) was added to a glass tube and the solvent was evaporated. Then, 5 mM MβCD solution in Ham's F-12 medium without serum was added to the dried cholesterol. The tube was vortexed, sonicated, and incubated overnight in a shaking bath at 37°C. MβCD was saturated with cholesterol at a MβCD/cholesterol molar ratio of 8:1, the saturation limit of MβCD (Christian et al., 1997). In preparation for an experiment, cells were washed three times with serum-free F-12 medium. Cells were then incubated with cholesterol-saturated MβCD solution or with MβCD solution containing no cholesterol (empty MβCD), or a mixture of these for 120 min. During the incubation, cells were maintained in a humidified CO_2 incubator at 37°C. After exposure to MβCD, cells were washed three times with serum-free medium and returned to the incubator. Cells that were incubated in serum-free medium maintained the elevated or the decreased level of cholesterol for at least 24 h, providing the time window for the electrophysiological recordings. To attain the intermediate cellular levels of cholesterol, cells were exposed to various mixtures of 5 mM MβCD saturated with cholesterol and 5 mM MβCD. MβCD and cholesterol were purchased from Sigma Chemical (St. Louis, MO).

Measurement of cellular sterols

Lipid was extracted from the washed cell monolayer using isopropanol as previously described (McCloskey et al., 1987). Total sterol mass analysis was done by gas-liquid chromatography (GLC) as previously described (Ishikawa et al., 1974; Klansek et al., 1995). Briefly, before lipid extraction the medium was removed and the cells were dried in air. Dried cells were extracted with isopropanol containing a known amount of cholesteryl methyl ether as an internal standard. After 4 h, the extracts were dried under N_2 at 35°C, reextracted with tetrachloroethylene, dissolved in CS_2, and analyzed by GLC. Cell protein was determined on the lipid-extracted monolayer using a modification (Markwell et al., 1978) of the method of Lowry (Lowry et al., 1951). All mass values were normalized on the basis of cell protein.

Electrophysiological recording

Previously, we have shown that the onset of Kir current change is delayed for 2–4 h after manipulating the membrane sterol composition (Romanenko et al., 2002). Therefore, here we recorded the currents at least 4 h after the end of treatment of cells with MβCD or its complexes.

Ionic currents were measured using whole-cell and cell-attached configurations of the standard patch-clamp technique (Hamill et al., 1981). Pipettes were pulled (SG10 glass, 1.20 mm ID, 1.60 mm; part # FPENNU 1.20ID1.60OD, Richland Glass, Richland, NJ) to give a final resistance of 2–6 MΩ. These pipettes generated high-resistance seals without fire polishing. A saturated salt agar bridge was used as reference electrode. Currents were recorded using an EPC9 amplifier (HEKA Electronik, Lambrecht, Germany) and accompanying acquisition and analysis software (Pulse and PulseFit, HEKA Electronik, Lambrecht, Germany).

Whole-cell recordings

The external recording solution contained (in mM) 150 NaCl, 6 KCl, 10 HEPES, 1.5 $CaCl_2$, 1 $MgCl_2$, and 1 EGTA, pH 7.3. The pipette solutions contained (in mM) 145 KCl, 10 HEPES, 1 $MgCl_2$, 4 ATP, and 1 EGTA, pH 7.3. Current was monitored by 500-ms linear voltage ramps from −160 to +60 mV at an interpulse interval of 5 s. Kir2 inactivation was determined by using a two-pulse voltage protocol: 500-ms voltage pulses were applied from −180 to +60 mV with increments of 10 mV and immediately followed by 10-ms test pulses to −160 mV. The holding potential for both protocols was −60 mV. Pipette and whole-cell capacitances were automatically compensated. Whole-cell capacitance and series resistance were compensated and monitored throughout the recording. Rs was compensated by 60–90%, with the compensation being limited by the stability of the patch.

Single-channel recordings

Pipettes were pulled to smaller diameter and had resistances of 7–9 MΩ. Both the external recording and the pipette solutions contained (in mM) 156 KCl, 10 HEPES, 1.5 $CaCl_2$, 1 $MgCl_2$, 1 EGTA, pH 7.3. Channel activity was recorded in 1.6-s sweeps with a 0.1-ms sampling interval and filtered at 500 Hz. All experiments were performed at room temperature (22–25°C). The chemicals for the recording solutions were obtained from Fisher Scientific (Fairlawn, NJ) or Sigma Chemical (St. Louis, MO). The osmolarities of all solutions were determined immediately before recording with a vapor pressure osmometer (Wescor, Logan, UT) and were adjusted by the addition of sucrose to attain isosmotic conditions.

To test if the inhibition of protein synthesis can affect the regulation of Kir2.1 current by cholesterol, the cells were transfected with one of the channel constructs, then, 24 h later, incubated overnight (12–18 h) with 5 μg/ml cycloheximide (CHX). Subsequently, the cells were treated for cholesterol depletion and the currents were recorded ≥4 h later (all the

solutions were supplemented with 5 μg/ml CHX). CHX was purchased from Sigma and 5 mg/ml CHX aqueous stock solution was used.

Immunoblotting and immunostaining

For immunoblots, cells were transfected with Kir2.x subunits and exposed to MβCD treatment, as described above, 24 h after the transfection. At 4 h after the MβCD treatment, the cells ($1–10 \cdot 10^6$) were washed three times with ice-cold phosphate-buffered solution (PBS) without Ca^{2+} and Mg^{2+}. All the following steps were carried out at 4°C. For preparation of whole-cell homogenate, washed cells were scraped into Laemmli buffer supplemented with 1x protease inhibitor cocktail (PIC) (Roche, Indianapolis, IN) and 1 μg/ml pepstatin, and sonicated. Alternatively, cells were scraped into Buffer A (in mM): 150 NaCl, 20 HEPES, 5 EDTA, pH 7.4, 1x PIC, 1 μg/ml pepstatin; homogenized in a Dounce tissue grinder (40 strokes), and centrifuged for 10 min at $1000 \times g$. The pellet was resuspended in Buffer A, dounced, and recentrifuged for 10 min at $1{,}000 \times g$. Combined supernatant was centrifuged for 1 h at $200{,}000 \times g$ (SW40Ti rotor, Beckman Coulter, Fullerton, CA). For preparation of total-membrane sample, the high-speed pellet was resuspended in Laemmli buffer and sonicated. Alternatively, for preparation of Triton-soluble and insoluble membrane fractions, the high-speed pellet was resuspended in 1 ml of Buffer A, sonicated 3×10 s, and supplemented with a small volume of concentrated solution of Triton X-100 to a final concentration of 1%. After 15 min incubation on ice the suspension was centrifuged for 1 h at $200{,}000 \times g$. Then the pellet was resuspended in Laemmli buffer. Sample total protein was measured using BCA Protein Assay kit (BioRad, Hercules, CA). Samples (1–50 μg protein/lane, identical amount per lane on a blot) were resolved with 12% SDS PAGE at reducing conditions followed by transfer to polyvinylidene difluoride membranes (Amersham, Piscataway, NJ). The membranes were probed with either anti-Kir2.x or anti-caveolin1 (BD Pharmingen, San Diego, CA). Bound primary antibodies were detected using secondary antibodies conjugated with HRP (Jackson Laboratories, West Grove, PA). Finally, immunoreactivity was visualized with ECL Plus reagent (Amersham, Piscataway, NJ). Detected bands were analyzed densitometrically using National Institutes of Health's ImageJ image processing program (available at http://rsb.info.nih.gov/ij/docs/index.html).

Affinity-purified rabbit anti-rat Kir2.2 polyclonal antibodies as previously described (Raab-Graham and Vandenberg, 1998) were generated to a peptide (RTNRYSIVSSEEDGMKLA) corresponding to a stretch of 21 amino acids in the carboxyl terminus of rat Kir2.2 (residues 390–410). Similarly, anti-rat Kir2.1 and Kir2.3 antibodies were made against amino acid sequences 390–411 and 2–19 from corresponding channel proteins.

For immunostaining, cells were transfected with HA-Kir2.1 construct and exposed to MβCD treatment, as described above, 48 h after the transfection. At 4 h after the MβCD treatment, HA-Kir2.1 transfected cells seeded on glass coverslips were fixed with 4% paraformaldehyde. Cells were then blocked (in PBS containing 1% bovine serum albumin (BSA) and 5% goat serum) for 1 h, incubated with primary antibody (1:100 in PBS containing 1% BSA and 5% goat serum) overnight, washed, incubated with Alexa586-conjugated secondary antibody (1:200 dilution in PBS containing 1% BSA and 1% goat serum, 1 h), washed, mounted, and viewed using a Zeiss Axiovert 100TV microscope (Zeiss, Jena, Germany). The primary antibody used was rat monoclonal anti-HA Ab3F10 (Roche Diagnostics, Germany) and the secondary antibody used was Alexa568-conjugated goat anti-rat IgG (Molecular Probes, Eugene, OR).

ELISA assay

The protocol for the ELISA assay was similar to that used for immunostaining with a few exceptions. Cells were seeded on glass coverslips in 24-well plates at a density of 2×10^5 cell/well, transfected, treated with MβCD, fixed, and incubated in primary antibody. Cells were then incubated with horseradish peroxidase (HRP) conjugated secondary antibody (1:200 dilution in PBS containing 1% BSA and 1% goat serum, 30 min) and washed in PBS containing 1% BSA and 1% goat serum, three times for 5 min each; then in PBS, three times for 5 min each). ECL Plus reagent (0.3 ml; Amersham, Piscataway, NJ) was then added to a well, and after 10 s measurements were taken on a Fluoroskan Ascent FL (Labsystems, Franklin, MA), with subsequent measurement taken every 30 s for a period of 2 min. The secondary antibody used was HRP-conjugated goat anti-rat (Jackson Laboratories, West Grove, PA).

Microscopy

Fluorescent images were acquired using a Zeiss Axiovert 100TV microscope with 63× Plan-Apochromat lens (NA 1.4), a precisely controlled XYZ stage (Applied Precision, Issaquah, WA) and a scientific-grade cooled charge-coupled device camera (MicroMax, Princeton Instruments, Trenton, NJ). To create 3-D reconstructions of the cells, 20 optical sections were attained at a distance of 300 nm apart along the z axis per cell. Constrained iterative deconvolution and 3-D rendering were performed using Deltavision software, Softworx (Applied Precision) on a 02 R10000 RISC workstation (Silicon Graphics, Mountain View, CA).

Analysis

Statistical analysis of the data was performed using a standard two-sample Student's t-test assuming unequal variances of the two data sets. Statistical significance was determined using a two-tail distribution assumption and was set at 5% ($p < 0.05$).

For whole-cell recordings, to minimize the effect of capacitative artifact at the beginning of the voltage steps, the peak currents were determined 14 ms after the beginning of voltage protocols. The degrees of rectification were quantified by fitting voltage dependence of relative cord conductances (G_c) with single Boltzmann function: $G_c = 1/(1 + \exp((V - V_{0.5})/k))$, where k is the slope factor, V is the membrane potential, and $V_{0.5}$ is the voltage of half-maximal blocking. Relative chord conductance was defined as the conductance relative to that expected for an unrectified current (Shyng et al., 1996). Channel conductances were determined as $G = (V_M - V_0)/I_{inst}$, where V_0 is the calculated reversal potential and I_{inst} is the instantaneous current measured upon introduction of the voltage step.

Reversal potentials were determined as the intersection of the current-voltage relationship with the x axis. The liquid junction potentials for whole-cell experiments were determined using the Junction Potential Calculator in the pCLAMP package (Axon Instruments, Union City, CA) and used for correction of determined reversal potentials. (Note that the recordings presented at the figures were not corrected for the junction potential).

The time constants of voltage-dependent inactivation were measured by fitting to a single exponential function $V(t) = Ae^{-t/\tau}$ where A is the current amplitude and τ is the time constant. The fits were obtained with the Levenberg-Marquardt algorithm using PulseFit software (HEKA Electronik).

The slopes of current versus cholesterol relationships for Kir2.1 and Kir2.3 channels were calculated from combined data ($n = 3–9$ per concentration) of daily averages of currents ($n = 3–7$ cells per day) for each of the cholesterol conditions. The cholesterol concentrations for each condition were averaged ($n = 3–15$). Analysis of covariance (test for homogeneity of regression slopes) was used for comparison of linear regression slopes (http://faculty.vassar.edu/lowry/VassarStats.html).

Single-channel amplitudes were determined using all-point histograms and the unitary conductances were calculated from the slopes of the linear fits of the amplitudes measured at no fewer than three voltages between −140 and −60 mV. The open probabilities for recordings with multiple channels present in the patch were calculated as $P_o = I/(iN)$, where I is the mean current of the patch, i is the average unitary channel current, and N is the number of channels in the patch. Due to high open probability of the channels, recordings with more than four channels were not analyzed.

Single-channel events were analyzed using TAC/TACFit software (Bruxton, Seattle, WA).

RESULTS

Kir2.1 is effectively regulated by cellular cholesterol

To determine the effect of cholesterol on Kir2.1 channels, the channels were heterologously expressed in CHO cells, a null cell line that almost completely lacks inward K^+ current (see *inset* to Fig. 1 *A*). To identify successfully transfected cells, Kir2.1 was coexpressed with a fluorescent marker, GFP. As expected, most of the fluorescent cells that were cotransfected (~80%) presented typical inwardly rectifying K^+ currents (Fig. 1 *A*, *upper traces*) that were ~100-fold larger than the background currents in untransfected cells or the cells that were transfected with GFP alone. The reversal potential of the currents was -82 ± 3 mV (after correction for the liquid junction potential; $n = 12$), close to the value of the theoretical reversal potential for K^+ current, which is -81 mV under the given recording conditions.

Cholesterol level in CHO cells was manipulated by treating transfected cells with MβCD or MβCD saturated with cholesterol (MβCD-cholesterol). Similar to our earlier study in bovine aortic endothelial cells, exposing CHO cells to MβCD resulted in an ~50% decrease in cellular cholesterol, whereas exposing the cells to MβCD-cholesterol resulted in ~40% cholesterol enrichment (Fig. 1 *B*). Cholesterol depletion caused an increase in the current density of Kir2.1, whereas cholesterol enrichment resulted in current suppression. It is important to note that Kir2.1 currents in cholesterol-enriched cells were still ~10-fold higher than the background endogenous currents. The values of the reversal potentials for the three experimental cell populations were -84 ± 2 mV and -81 ± 3 mV for cholesterol-depleted cells ($n = 7$) and cholesterol-enriched cells ($n = 8$), respectively, similar to the value of the reversal potential in the untreated cells. Mean current densities for the three experimental cell populations are shown in Fig. 1 *C*. The inverse relationship between the current densities and cellular cholesterol level was not due to a change in the current rectification properties (Fig. 1 *D*) or changes in cell capacitance (13 ± 1, 12 ± 2, and 15 ± 1 pF for cholesterol-depleted, cholesterol-enriched, and control cells, respectively). Fig. 2 shows that an increase in cellular cholesterol had no effect on the unitary conductance of the Kir2.1 channels and had a very small effect on the channel open probability, clearly insufficient to account for the observed decrease in the whole-cell Kir2.1 current. Similarly, cholesterol enrichment also had no effect on the hyperpolarization-induced inactivation of the whole-cell Kir2.1 (Fig. 2, *C–E*).

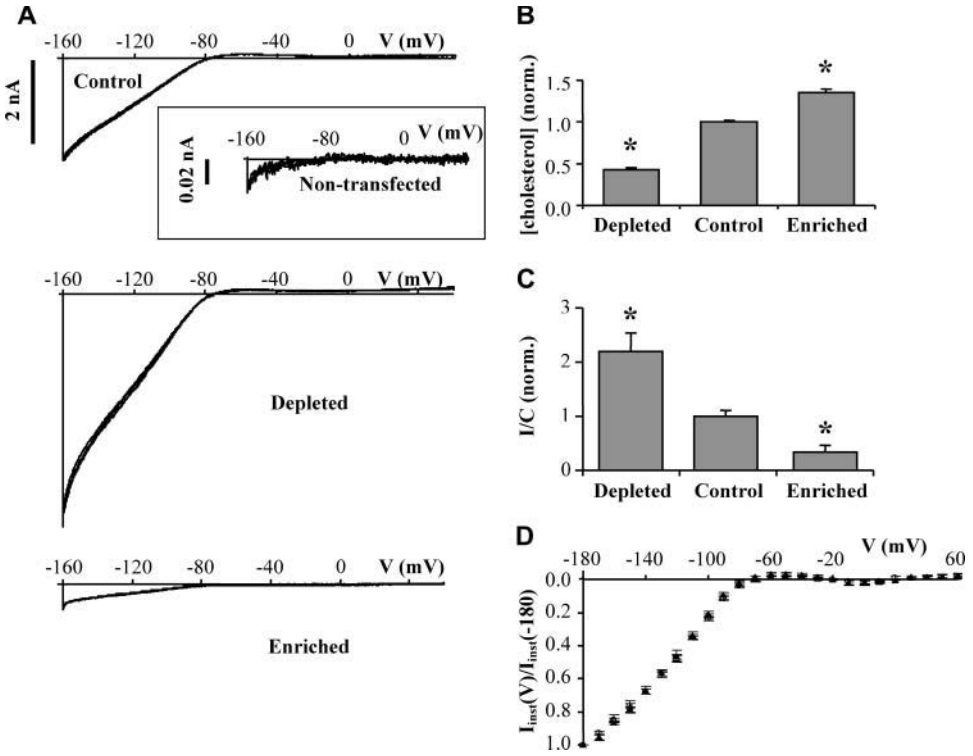

FIGURE 1 Kir2.1 currents in cells depleted of or enriched with cholesterol. (*A*) Typical Kir2.1 current traces recorded from three individual cells: a control cell that was exposed to serum-free medium alone (*upper family*); a cell depleted of cholesterol by exposure to 5 mM MβCD (*middle family*); and a cell that was enriched with cholesterol by exposure to 5 mM MβCD saturated with cholesterol (*lower family*). Three superimposed traces are shown for each cell. The currents were elicited by 500 ms linear voltage ramps from -160 mV to $+60$ mV, the ramps were applied with intervals of 5 s for the duration of the experiment. The holding potential between the ramps was -60 mV. The inset shows the background current in a nontransfected cell. (*B*) Cellular levels of cholesterol after treatment as in *A* measured by gas-liquid chromatography. Cholesterol levels after treatment of transfected and nontransfected cells were not different (not shown; $n = 9$–15, $^*P < 0.01$). (*C*) Peak current densities (-160 mV) of the three cell populations. Three to seven cells were patched per condition per day and the daily average was normalized to the same-day control. The bars represent the data pooled from 3–6 experimental days ($^*P < 0.01$). (*D*) Normalized current-voltage relationships at the three experimental conditions: (○), control cells; (■), cells treated with 5 mM MβCD; and (▲), cells treated with 5 mM MβCD-cholesterol (the symbols are mainly superimposed; $n = 4$–7).

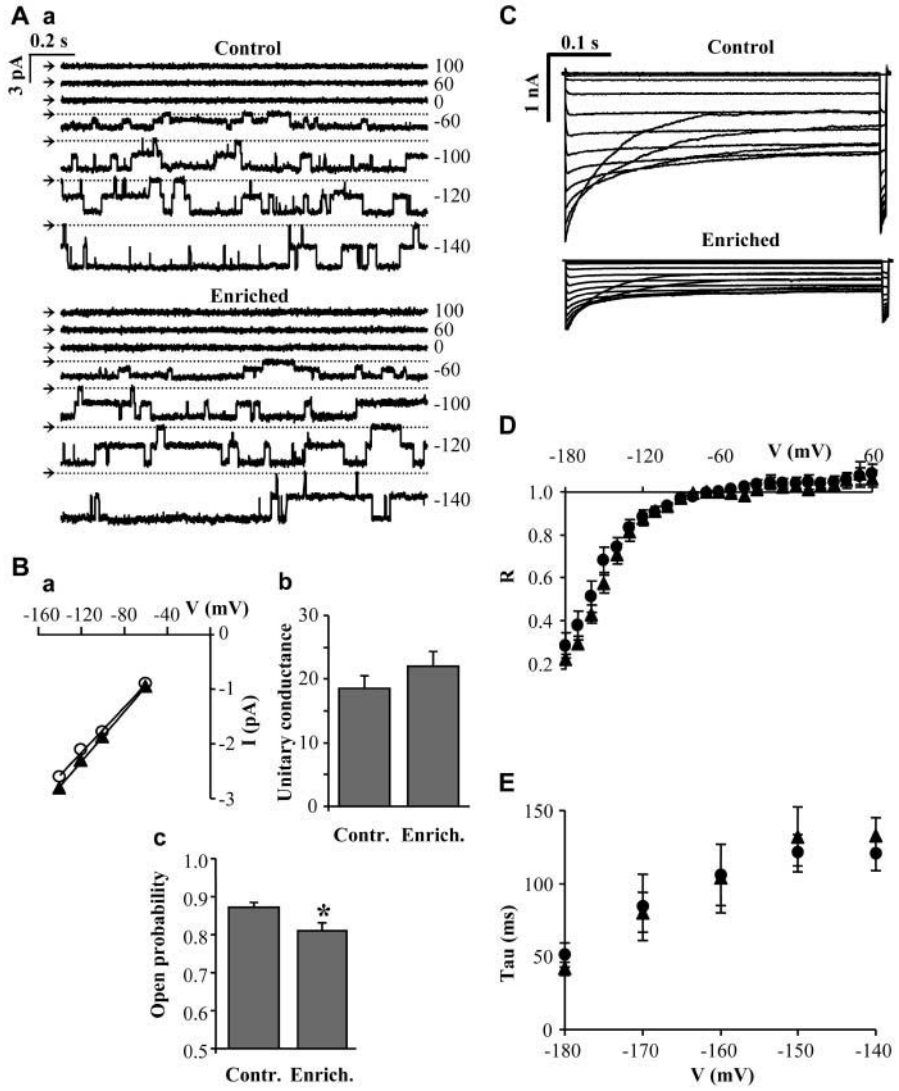

FIGURE 2 Nominal effect of cholesterol on Kir2.1 single-channel properties and whole-cell current inactivation. (*A*) Typical single-channel currents at different membrane potentials recorded in the cell-attached configuration recorded in a control cell (*a*) and in a cell treated with 5 mM MβCD-cholesterol (*b*). Bath and pipette solutions contained 156 mM K^+. The currents were recorded at 0.1-ms sample intervals and filtered at 500 Hz. The closed level is indicated by the arrow to the left of each trace and the broken line. (*Ba*) I/V relationships for the channels shown in *A*: (○), control cell; (▲), cell treated with 5 mM MβCD-cholesterol. (*Bb*) Average unitary conductances calculated from the slopes of the linear fits between −140 and −60 mV and (*Bc*) open probabilities at −60 mV determined in control and cholesterol-enriched cells (n = 22–34, $^*P < 0.05$). (*C*) Typical Kir2.1 current traces recorded from individual control and cholesterol-enriched cells. A two-pulse voltage protocol was used: 500-ms voltage steps from −180 to +60 mV with increments of 10 mV and immediately followed by 10-ms test pulses to −160 mV. (*D*) Inactivation ratio (*R*) was determined as the ratio of the current amplitude in response to a test voltage pulse to that of a +60 mV test voltage pulse: (●), control cells; (▲), cells treated with 5 mM MβCD-cholesterol (n = 6–9). (*E*) Time constant of inactivation (τ) were plotted against voltage (single exponential fit): (●), control cells; (▲), cells treated with 5 mM MβCD-cholesterol (n = 8–9).

Inhibition of protein synthesis does not abolish the upregulation of Kir2.1 by cholesterol depletion

One possible mechanism of how changes in the level of cholesterol might regulate Kir2.1 current would be regulation of protein synthesis. To test this possibility, 24 h after transfection with Kir2.1 and GFP the cells were incubated with CHX, a widely-used nonspecific protein synthesis inhibitor that has been shown to almost completely block protein synthesis within 4–8 h (e.g., Nolop and Ryan, 1990; Polunovsky et al. 1994). After overnight (12–18 h) exposure to 5 μg/ml CHX, the average current density of Kir2.1 decreased ~2.5-fold, as determined by comparing CHX-treated and control cells on the same day. As expected, when the cells were transfected in the presence of CHX, GFP fluorescence was not observed. CHX had no apparent effect on cell morphology or cell capacitance. The rectification of the Kir2.1 current was also unaffected, which was determined by comparing voltage dependences of relative cord conductances as described in Materials and Methods. $V_{0.5}$ was −82 ± 2 mV (n = 6) and −82 ± 1 mV (n = 4) for control cells and CHX-treated cells, respectively, and the slope factor (k) was 11 ± 1 (n = 6) and 11 ± 2 (n = 4) for the cell populations. Fig. 3 shows that although exposure to CHX decreased the amplitude of Kir2.1 current (Fig. 3 *A*), cholesterol depletion still effectively upregulated the current in CHX-treated cells (Fig. 3 *B*). Moreover, comparison of the current densities normalized to respective controls recorded on the same days showed that the sensitivity of Kir2.1 to cholesterol depletion was unaffected by the inhibition of protein synthesis.

Changes in cellular cholesterol have no effect on total Kir2.1 protein level

To test further whether the sensitivity of Kir2.1 to cholesterol involved regulation of the amount of Kir2.1 protein, the

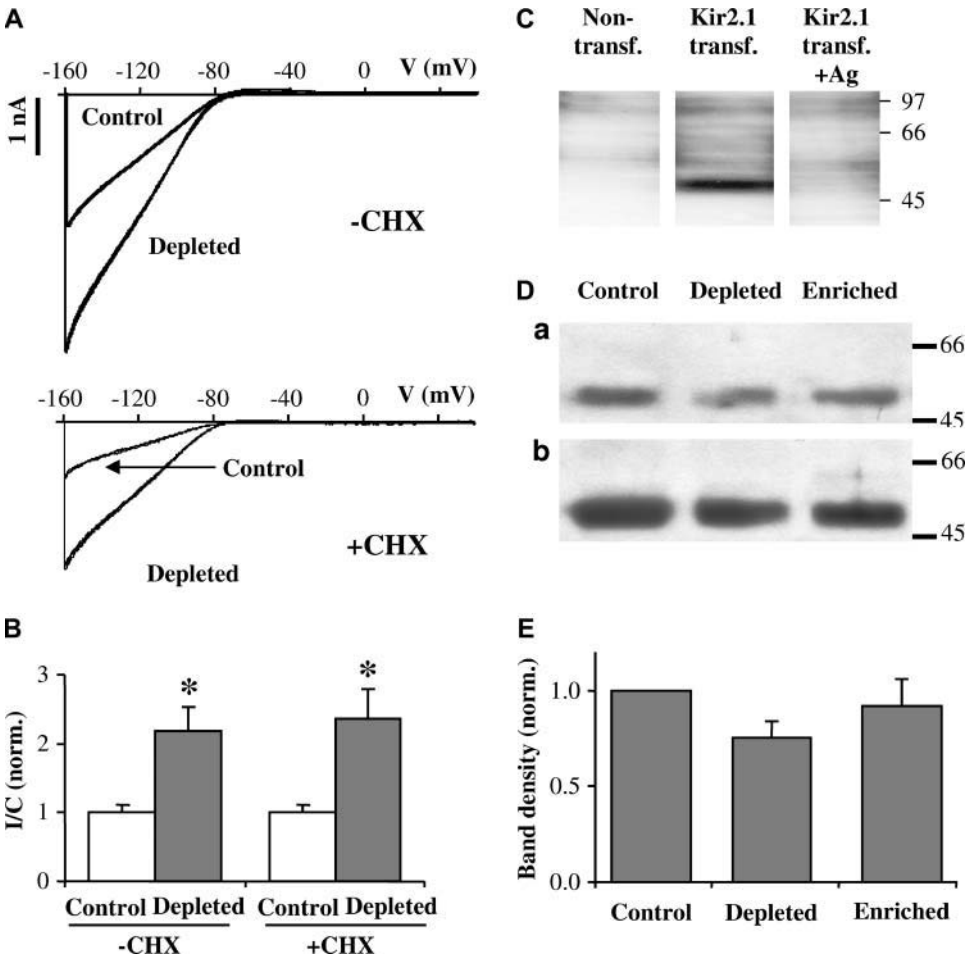

FIGURE 3 Cholesterol regulates Kir2.1 after blocking protein synthesis and does not affect Kir2.1 protein expression. (*A*) Typical current traces recorded from individual control cells or cells treated with 5 mM MβCD. The upper panel represents cells cultured in full medium before cholesterol depletion with MβCD and in serum-free medium after the treatment. The lower panel represents experiments for which cells were treated similarly except that all the media were supplemented with 5 μg/ml cycloheximide (+*CHX*) for a total time of exposure to the protein synthesis inhibitor of 18 h. (*B*) Mean peak current densities in control cells and cholesterol-depleted cells, which were either exposed or not exposed to CHX. The current densities were normalized to the average of current densities in control cells recorded on the same experimental day ($n = 3$ days, with 3–5 cells per day per condition; $^*P < 0.01$ compared to respective controls). (*C*) The specificity and sensitivity of anti-Kir2.1 antibodies were tested by probing the blots prepared either from nontransfected cells or from cells transfected with Kir2.1 cDNA. Additionally, a separate blot was probed with the antibodies preincubated with the antigen. For each lane, 10 μg of total protein was loaded. (*D*) An example of immunoblots of CHO cells expressing Kir2.1 that were exposed to serum-free medium, 5 mM MβCD, or 5 mM MβCD saturated with cholesterol. The blots were prepared from either (*a*) whole-cell homogenates (12 μg of total protein per lane), or (*b*) total membrane fraction (3 μg of total protein per lane). To avoid known saturating artifacts of high chemiluminescent signals, only the images that were well below saturating levels were chosen for the quantification. (*E*) Mean band densities of Kir2.1 immunoblots described in *Da* ($n = 4$).

levels of Kir2.1 protein were compared under different cholesterol conditions using Western blot analysis. Kir2.1 proteins were probed with a polyclonal antibody raised against rat Kir2.1. As expected, CHO cells transfected with Kir2.1 presented a prominent band at ~50 kDa (Kir2.1 molecular mass predicted from its primary structure is 48), whereas nontransfected CHO cells do not show this band. As a demonstration of the specificity of this immunoreactivity, the band disappeared after preabsorption of the antibody with the antigen (Fig. 3 *C*). Fig. 3 *D* shows examples of blots obtained by probing preparations of whole-cell homogenates (*a*) or total membrane fractions (*b*) under different cholesterol conditions. The intensities of the bands were similar in cholesterol-depleted, cholesterol-enriched, and control cells. Densitometric analysis of the bands shows no statistical difference in Kir2.1 levels under the different cholesterol conditions (Fig. 3 *E*). Since cholesterol depletion resulted in rounding up of a small fraction of cells, a slight decrease in the band density in cholesterol-depleted cells was likely to be a consequence of the loss of cells during sample preparation.

Cholesterol level has no effect on surface expression of Kir2.1

To determine whether changes in the level of cholesterol affect the surface expression of Kir2.1 channels, the cells were transfected with Kir2.1 subunits tagged with hemagglutinin (HA) epitope (YPYDVPDYA) on the extracellular domain. The rationale of this approach is that the channels that are inserted into the plasma membrane will have the tag accessible for the anti-HA antibodies without permeabilization of the membrane, whereas channels that reside in the intracellular membranes will not. This method, therefore, allows us to assess the surface expression of the channels and to estimate whether cholesterol modulates the surface expression of Kir2.1 channels. Two approaches were used for quantification of HA-Kir2.1 surface expression: 1), deconvolution microscopy to estimate the surface expression of the channels at a single-cell level (Fig. 4, *A* and *B*); and 2), ELISA to measure the surface expression of the channels at a cell population level (Fig. 4 *C*).

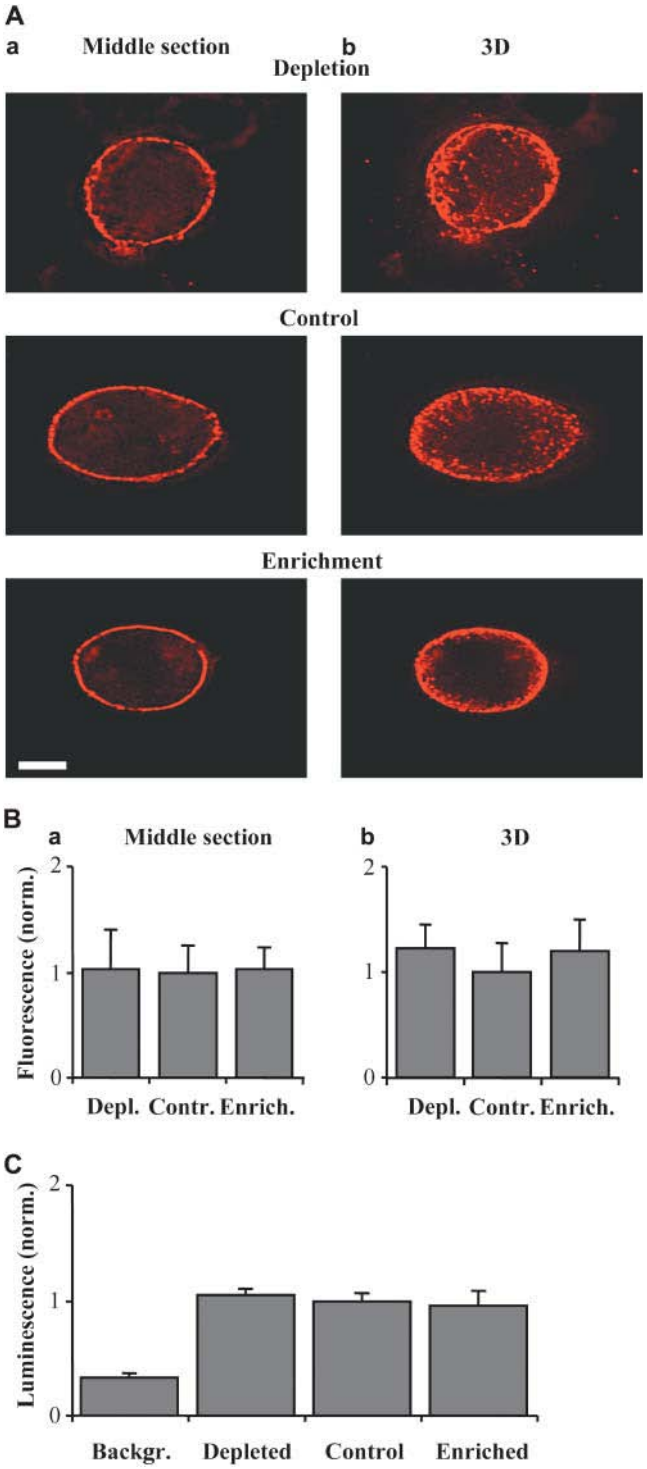

FIGURE 4 Effect of cholesterol modulation on surface expression of Kir2.1. (*Aa*) Typical images of Kir2.1 surface expression observed in the middle plane of cells after cholesterol depletion, no treatment, and cholesterol enrichment. Bar, 4 μm. (*Ab*) 3-D reconstruction of the cells shown in *Aa*, which combines 20 optical sections taken at 300 nm apart. (*B*) Quantification of Kir2.1 surface expression at the middle plane (*a*) and in 3-D reconstructed images (*b*) of single cells. Expression levels were determined as a function of fluorescently labeled HA-Kir2.1 intensity in cholesterol-depleted, control, and cholesterol-enriched cells ($n = 10$ per condition). Fluorescent intensity of each cell was normalized to its area. There was statistically no difference in Kir2.1 surface expression at the middle plane as well as the upper and lower sections (not shown) for each cholesterol condition. Identical results were obtained in four independent experiments. (*C*) Surface expression of Kir2.1 in a cell population was determined as a function of luminescence using ELISA assay. In each experiment luminescence was measured in quadruplicate for each cholesterol condition. No statistical difference in Kir2.1 expression was confirmed in four independent experiments.

Fig. 4 shows that neither cholesterol depletion nor cholesterol enrichment had any significant effect on the HA-Kir2.1 surface expression. Typical images of optical middle sections and of 3-D reconstructions composed of 20 individual sections each of nonpermeabilized CHO cells under different cholesterol conditions are shown in Fig. 4 *A*, panels *a* and *b*, respectively. No detectable fluorescence was observed in cells exposed to secondary antibodies only (not shown). HA-specific fluorescence appeared more clearly in the edge of the cells, as compared to the top and bottom surfaces, because imaging through the edges of rounded cells provides better visualization of the cell sides. Fig. 4 *B* shows that altering cell cholesterol level had no effect on HA-specific fluorescence of individual cells. Fluorescence was quantified for the middle sections (Fig. 4 *B*, panel *a*) and for the 3-D projections (Fig. 4 *B*, panel *b*), as well as for upper and lower surface sections of the same cells (not shown). Similar results were obtained in four independent experiments.

To quantitatively determine the surface expression level of Kir2.1 in cell populations ($\sim 3 \times 10^5$ cells/sample), HA-Kir2.1 expression was quantified using an ELISA assay. Consistent with the results obtained from the analysis of individual cells, luminescence level measured in quadruplicate samples per condition (Fig. 4 *C*) was similar at all cholesterol levels in four independent experiments.

Comparison of cholesterol sensitivity of Kir2.1 with the other Kir2.x channels

The subfamily of Kir2 channels consists of four members, Kir2.1–Kir2.4, whose homology differs between ~70% and ~50%. Therefore, we compared the inhibitory effect of cholesterol on the four channels expressed in CHO cells. All four channels were successfully expressed in the CHO cells presenting typical inwardly rectifying K^+ currents with the predicted values of the reversal potentials (Fig. 5 *A*). Although all Kir2.x were significantly lower in cholesterol-enriched cells in comparison with control cells, the degree of the current decrease was different. Specifically, Kir2.1 and Kir2.2 currents were strongly suppressed (~70% inhibition), whereas Kir2.3 was significantly less suppressed (~30% inhibition) by cholesterol. For the high-amplitude Kir2.1 and Kir2.2 control currents, the current amplitudes may be

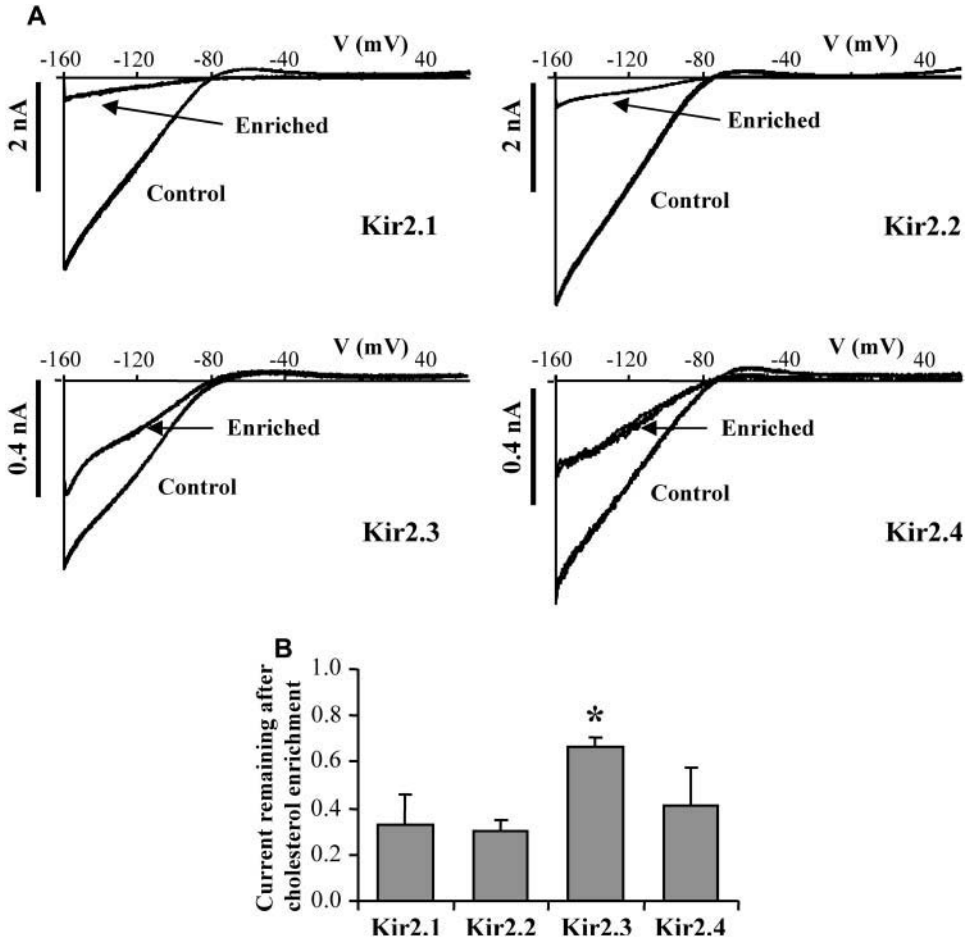

FIGURE 5 The differential sensitivity of heterologous Kir2.x channels to cholesterol enrichment. (*A*) Each panel shows typical current traces recorded from individual cells expressing the indicated Kir2.x channel that were either exposed to serum-free medium (control) or to 5 mM MβCD saturated with cholesterol. (*B*) Mean current densities in cholesterol-enriched cells normalized to respective currents in control cells. The data were pooled from 3–8 experimental days (*$P < 0.05$ compared to Kir2.1 and Kir2.2).

slightly underestimated due to incomplete compensation of the pipette series resistance, suggesting that the degree of current suppression by cholesterol for Kir2.1 and Kir2.2 is higher than measured. The actual difference between the sensitivities of these channels and Kir2.3 channels to cholesterol is expected, therefore, to be greater than estimated from the recordings. Rectification properties of none of the channels were affected by the cholesterol treatment (not shown).

To investigate further the difference between cholesterol sensitivities of Kir2.1 and Kir2.3, the currents were recorded in cells in which cholesterol was varied over the range between 60% depletion and 40% enrichment. This was achieved by exposing the cells to the mixture of MβCD and MβCD-cholesterol complex at different ratios, which effectively resulted in changing the ratio between MβCD and cholesterol. As was shown earlier (Christian et al., 1997), this procedure allowed precise adjustment of the cellular cholesterol to different levels (Fig. 6 *A*). Over this range, the relationship between the current densities and the level of cellular cholesterol was linear for both Kir2.1 and Kir2.3. The slopes of the regression of the normalized data were -2.0 ± 0.3 and -0.8 ± 0.2 for Kir2.1 and Kir2.3, respectively ($p < 0.01$), demonstrating the strong difference in the cholesterol sensitivities of Kir2.1 and Kir2.3 channels (Fig. 6 *B*). However, the inactivation properties of Kir2.1 (Fig. 2) and Kir2.3 (not shown) were similar and unaffected by cholesterol.

Localization of Kir2.x channels in detergent-resistant membranes

Sensitivity of the Kir2.x to cholesterol depletion suggested that these channels might partition into lipid rafts, cholesterol-rich detergent-resistant membrane domains. One of the common methods used to determine whether the proteins partition into lipid rafts is to solubilize nonlipid raft membranes with Triton X-100 and test the distribution of the protein between the Triton-soluble and Triton-insoluble membrane fractions. Kir2.1, Kir2.2, and Kir2.3 almost completely partitioned to Triton-insoluble membrane fractions (the antibody for Kir2.4 was not available to us), which contained ~25% of total membrane protein. Specifically, Fig. 7 shows Kir2.x-specific bands in whole cell, total membrane, and its Triton-soluble and Triton-insoluble fractions. Each individual blot was also probed for caveolin,

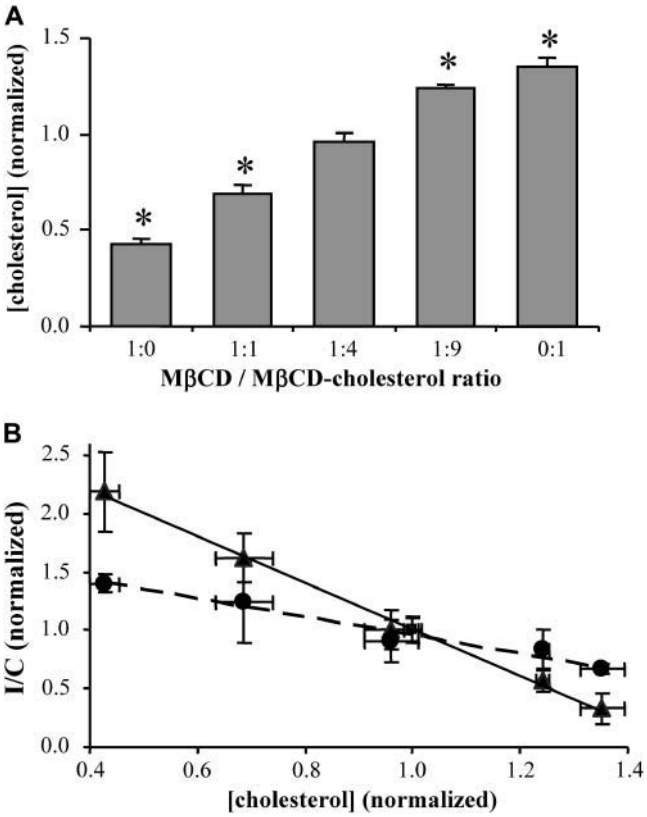

FIGURE 6 The functional dependence of Kir2.1 and Kir2.3 currents on the level of membrane cholesterol. (*A*) Cellular levels of free cholesterol in cells exposed to mixtures with various ratios of MβCD to MβCD-cholesterol (n = 6–9, *$P < 0.05$). (*B*) Normalized peak current densities (−160 mV) were plotted as a function of normalized level of free cholesterol in cells exposed to mixtures of 5 mM MβCD and 5 mM MβCD-cholesterol. All peak current densities were normalized to those of control cells measured on the same day (3–6 cells per day per condition): (▲), Kir2.1; (●), Kir2.3 (n = 3–10 experimental days). The data were adequately fit by linear regression analysis ($r^2 \geq 0.99$ for Kir2.1 and $r^2 \geq 0.96$ for Kir2.3).

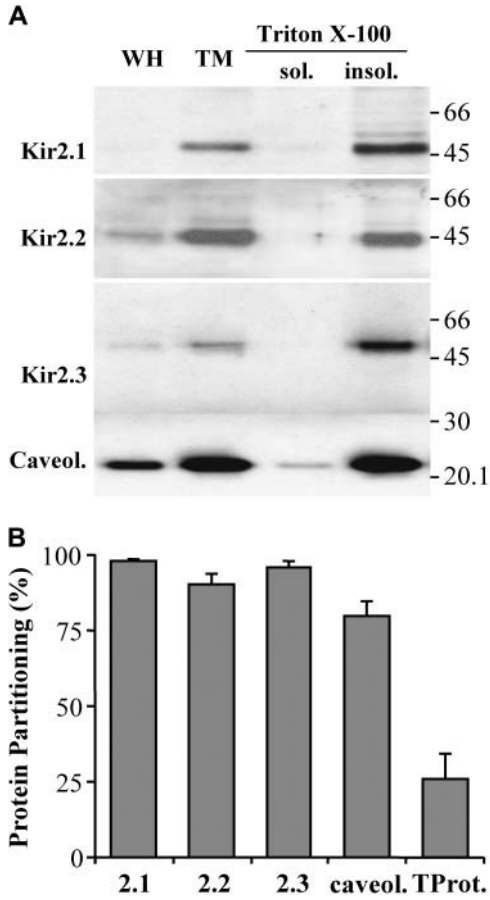

FIGURE 7 Partitioning of heterologous Kir2.x in to Triton X-100-insoluble membrane fraction. (*A*) An example of typical immunoblots prepared from CHO cells expressing Kir2.1, Kir2.2, and Kir2.3 channels. Caveolin was usually detected simultaneously with the individual channel on the membrane portion that was cut below 45 kDa. The vertical lanes represent samples prepared from whole-cell homogenates (*WH*), total membrane fraction (*TM*), Triton-soluble (*sol.*) and Triton-insoluble (*insol.*) fractions. The samples were loaded with the same amount of total protein. (*B*) The percentage of the channel proteins and caveolin (*caveol.*), and total protein (*TProt.*) associated with Triton-insoluble membrane fractions ($n = 4$).

a major lipid raft marker. The distribution of Kir2.x-specific bands between the Triton-soluble and insoluble fractions strongly correlated with the distribution of caveolin. The partitioning of the Kir2.x channels and of caveolin was quantified by calculating the ratio of the band density in Triton-insoluble fraction to the total amount of the protein in both membrane fractions (Fig. 7 *B*).

DISCUSSION

Growing evidence suggest that ion channels are regulated by their lipid environment (reviewed by Barrantes, 2002; Hilgemann et al., 2001; Martens et al., 2004; and Tillman and Cascio, 2003). Specifically, multiple studies demonstrated that inwardly rectifying K^+ channels are regulated by phosphoinositides (Cukras et al., 2002; Lopes et al., 2002; Rohacs et al., 1999; Shyng et al., 2000). In addition, it was shown that an increase in membrane cholesterol suppresses large conductance Ca^{2+}-sensitive K^+ channels (Bolotina et al., 1989; Chang et al., 1995) and shifts the voltage dependence of several subtypes of voltage-gated K^+ channels (Hajdu et al., 2003; Martens et al., 2000, 2001). Our recent study showed that cholesterol also regulates inwardly rectifying Kir current (Romanenko et al., 2002) but the molecular identity of the cholesterol-sensitive Kir has not been established and little was known about the mechanisms responsible for this effect. In this study, we demonstrate that Kir2.x channels heterologously expressed in a null cell line are cholesterol sensitive and we investigate the mechanisms that might be responsible for this effect. Our data suggest that cholesterol specifically alters the activity of plasma membrane Kir2 channels and modulates transitions from active to ''silent'' states of the channels.

First, we tested whether cholesterol-induced suppression of Kir2.1 current can be accounted for by changes in the

single-channel properties, as was shown previously for large-conductance Ca^{2+}-sensitive K^+ channels in smooth muscle cells (Bolotina et al., 1989; Chang et al., 1995). Our observations show, however, that changes in the level of cellular cholesterol had no effect on the unitary conductance and only a very small effect on the open probability of Kir2.1 (~7% decrease in P_o), demonstrating that changes in the single-channel properties cannot account for cholesterol-induced suppression of Kir2.1. These observations are consistent with our earlier data showing no effect of cholesterol on the single-channel properties of endogenous Kir current in aortic endothelial cells (Romanenko et al., 2002). It is also consistent with a lack of cholesterol effect on the biophysical properties of the whole-cell Kir2.1 current.

Second, we tested the hypothesis that cholesterol may suppress the expression of the channels. The rationale for this hypothesis was that cholesterol is well-known to regulate the expression of a variety of proteins (reviewed by Shimano, 2001). Although it has already been shown that, in contrast to Kir3.1 and Kir6.2, hypercholesterolemia has no effect on Kir2.1 mRNA in smooth muscle cells (Ren et al., 2001), the effect of cholesterol on the protein level of Kir2.1 has not been tested. It is particularly important because it is known that mRNA levels may not necessarily precisely reflect the cellular levels of the proteins (Barry et al., 1995). Here we show that 1), sensitivity of the current to cholesterol was retained after protein synthesis was blocked by CHX; and 2), changes in the level of cholesterol had no apparent effect on the level of the protein as compared by immunoblotting, indicating that regulation of protein expression is not responsible for the cholesterol sensitivity of the Kir2.1 current. Taken together with the observation that cholesterol has no effect on the single-channel properties of the channels, these observations suggest that changes in the level of cellular cholesterol affect the number of channels in the plasma membrane.

Finally, we tested the possibility that changes in the level of cholesterol affect the surface expression of the channels, so that more channels are retained in the intracellular membranes and fewer channels are inserted into the plasma membrane. Indeed, cholesterol-rich membrane domains are known to have a major impact on sorting and trafficking of the membrane proteins (for review, see Ikonen, 2001). However, no cholesterol effect on the surface expression of Kir2.1 channels was observed in our study indicating that cholesterol-induced regulation of Kir2.1 is not due to the regulation of insertion/retrieval of the channels to and from plasma membrane. It is noteworthy that, consistent with the lack of cholesterol effect on Kir2.1 surface expression, there was also no effect on cell capacitance supporting our conclusion that downregulation of the current is not due to the retrieval of the channels from the plasma membrane. This indicates that an increase in membrane cholesterol decreases the number of active Kir2.1 channels without decreasing the total number of the channels in the plasma membrane. This observation is also consistent with cholesterol having an all-or-nothing effect on a single-channel level, whereas on the level of the whole-cell channel population the effect is graded. We propose, therefore, that an increase in membrane cholesterol induces a conformation change of the channel protein that leads to a ''silent'' (nonactive) state of the channel. Silent channels are retained on the plasma membrane but cannot be detected by single-channel analysis.

Interestingly, Kir2.1 and Kir2.2 were significantly more strongly inhibited by cholesterol than Kir2.3, whereas Kir2.4 had intermediate cholesterol sensitivity. This result implies that structural differences between the channels are important for their cholesterol sensitivity. The overall homology between Kir2.1/Kir2.2 and Kir2.3 channels is 60–70%, and several regulatory sites were found to be different in these channels (Coulter et al., 1995; Zhu et al., 1999). It is also noteworthy that Kir2.1, Kir2.2, and Kir2.3 channels were found to partition virtually exclusively into Triton-insoluble domains. Similar observations were reported recently for Kir2.1 channels (Stockklausner and Klocker, 2003) and for voltage-gated K^+ channels (Martens et al., 2000, 2001). This is the first report that Kir2.2 and Kir2.3 partition into detergent-resistant membrane fractions suggesting that this is a general feature of Kir2.x subunits. Although it is known that resistance to detergent solubilization does not automatically equate to localization to lipid rafts in living cells (Munro, 2003), the facts that all the Kir2.x subunits partitioned to the detergent-resistant fraction and showed functional changes induced by perturbations of membrane cholesterol are suggestive that the sterol content in the immediate membrane microenvironment regulates channel activity. It is also important to note that since the channels were observed almost exclusively in Triton-insoluble fractions under the control conditions, it is unlikely that cholesterol-induced suppression of the current can be due to further partitioning of the channels into lipid raft domains. Since alterations of sterol levels can dramatically affect the stability of rafts (Kabouridis et al., 2000, Simons and Toomre, 2000), we suggest that changes in the level of cellular cholesterol alter the channel activity by modifying the interactions of the channels with the protein or lipid components of lipid rafts.

The authors thank Dr. Yoshihisa Kurachi, Dr. Andreas Karschin, Dr. Caroline Dart, and Dr. Scott L. Diamond for the gifts of Kir2.1, Kir2.2, Kir2.4, and eGFP DNA. We also thank Dr. Peter F. Davies and other colleagues at the Institute for Medicine and Engineering for advice and valuable discussions.

This work was supported by the American Heart Association (AHA) Scientist Development grant 0130254N (to I.L.), the AHA postdoctoral fellowship 0225412U (to V.G.R), California Tobacco-related Disease Research Program 11RT-0114 (to C.A.V.), and the National Institutes of Health grants HL073965-01A1 (to I.L.), HD-045664 (to A.J.T. and I.L.), HL22633 and HL63768 (to G.R.), NS43377 (to C.A.V.), and HL64388-01A1 (to Dr. Peter Davies).

REFERENCES

Barrantes, F. J. 2002. Lipid matters: nicotinic acetylcholine receptor-lipid interactions (Review). *Mol. Membr. Biol.* 19:277–284.

Barry, D. M., J. S. Trimmer, J. P. Merlie, and J. M. Nerbonne. 1995. Differential expression of voltage-gated K+ channel subunits in adult rat heart. Relation to functional K+ channels? *Circ. Res.* 77:361–369.

Beuckelmann, D. J., M. Nabauer, and E. Erdmann. 1993. Alterations of K+ currents in isolated human ventricular myocytes from patients with terminal heart failure. *Circ. Res.* 73:379–385.

Bolotina, V., V. Omelyanenko, B. Heyes, U. Ryan, and P. Bregestovski. 1989. Variations of membrane cholesterol alter the kinetics of Ca^{2+}-dependent K^+ channels and membrane fluidity in vascular smooth muscle cells. *Pflugers Arch.* 415:262–268.

Chang, H. M., R. Reitstetter, R. P. Mason, and R. Gruener. 1995. Attenuation of channel kinetics and conductance by cholesterol: an interpretation using structural stress as a unifying concept. *J. Membr. Biol.* 143:51–63.

Christian, A. E., M. P. Haynes, M. C. Phillips, and G. H. Rothblat. 1997. Use of cyclodextrins for manipulating cellular cholesterol content. *J. Lipid Res.* 38:2264–2272.

Coulter, K. L., F. Perier, C. Radeke, and C. Vandenberg. 1995. Identification and molecular localization of a pH-sensing domain for the inward rectifier potassium channel HIR. *Neuron.* 15:1157–1168.

Cukras, C. A., I. Jeliazkova, and C. G. Nichols. 2002. Structural and functional determinants of conserved lipid interaction domains of inward rectifying Kir6.2 channels. *J. Gen. Physiol.* 119:581–591.

Dart, C., and M. L. Leyland. 2001. Targeting of an A Kinase-anchoring protein, AKAP79, to an inwardly rectifying potassium channel, Kir 2.1. *J. Biol. Chem.* 276:20499–20505.

Eschke, D., M. Richter, E. Brylla, A. Lewerenz, K. Spanel-Borowski, and K. Nieber. 2002. Identification of inwardly rectifying potassium channels in bovine retinal and choroidal endothelial cells. *Ophthalmic Res.* 34: 343–348.

Forsyth, S. E., A. Hoger, and J. H. Hoger. 1997. Molecular cloning and expression of a bovine endothelial inward rectifier potassium channel. *FEBS Lett.* 409:277–282.

Hajdu, P., Z. Varga, C. Pieri, G. Panyi, and R. Gaspar, Jr. 2003. Cholesterol modifies the gating of Kv1.3 in human T lymphocytes. *Pflugers Arch.* 445:674–682.

Hamill, O. P., A. Marty, E. Neher, B. Sakmann, and F. J. Sigworth. 1981. Improved patch-clamp techniques for high-resolution current recording from cells and cell-free membrane patches. *Pflugers Arch.* 391:85–100.

Hilgemann, D. W., S. Feng, and C. Nasuhoglu. 2001. The complex and intriguing lives of PIP2 with ion channels and transporters. *Sci. STKE.* 111:RE19.

Hille, B. 1992. Ionic Channels of Excitable Membranes. Sinauer Associates, Sunderland, MA.

Hosaka, Y., H. Hanawa, T. Washizuka, M. Chinushi, F. Yamashita, T. Yoshida, S. Komura, H. Watanabe, and Y. Aizawa. 2003. Function, subcellular localization and assembly of a novel mutation of KCNJ2 in Andersen's syndrome. *J. Mol. Cell. Cardiol.* 35:409–415.

Huang, C. L., S. Feng, and D. W. Hilgemann. 1998. Direct activation of inward rectifier potassium channels by PIP2 and its stabilization by GBY. *Nature.* 391:803–806.

Ikonen, E. 2001. Roles of lipid rafts in membrane transport. *Curr. Opin. Cell Biol.* 13:470–477.

Ishikawa, T. T., J. MacGee, J. A. Morrison, and C. J. Glueck. 1974. Quantitative analysis of cholesterol in 5 to 20 μL of plasma. *J. Lipid Res.* 15:286–291.

Jongsma, H. J., and R. Wilders. 2001. Channelopathies: Kir2.1 mutations jeopardize many cell functions. *Curr. Biol.* 11:R747–R750.

Kabouridis, P. S., J. Janzen, A. L. Magee, and S. C. Ley. 2000. Cholesterol depletion disrupts lipid rafts and modulates the activity of multiple signaling pathways in T lymphocytes. *Eur. J. Immunol.* 30:954–963.

Kamouchi, M., K. Van Den Bremt, J. Eggermont, G. Droogmans, and B. Nilius. 1997. Modulation of inwardly rectifying potassium channels in cultured bovine pulmonary artery endothelial cells. *J. Physiol.* 504: 545–556.

Karkanis, T., S. Li, J. G. Pickering, and S. M. Sims. 2003. Plasticity of KIR channels in human smooth muscle cells from internal thoracic artery. *Am. J. Physiol. Heart Circ. Physiol.* 284:H2325–H2334.

Klansek, J., P. Yancey, R. W. St. Clair, R. T. Fisher, W. J. Johnson, and J. M. Glick. 1995. Cholesterol quantification by GLC: artifactual formation of short-chain steryl esters. *J. Lipid Res.* 36:2261–2266.

Kubo, Y., T. J. Baldwin, Y. N. Jan, and L. Y. Jan. 1993. Primary structure and functional expression of a mouse inward rectifier potassium channel. *Nature.* 362:127–132.

Lange, P. S., F. Er, N. Gassanov, and U. C. Hoppe. 2003. Andersen mutations of KCNJ2 suppress the native inward rectifier current IK1 in a dominant-negative fashion. *Cardiovasc. Res.* 59:321–327.

Levitan, I., A. E. Christian, T. N. Tulenko, and G. H. Rothblat. 2000. Membrane cholesterol content modulates activation of volume-regulated anion current (VRAC) in bovine endothelial cells. *J. Gen. Physiol.* 115:405–416.

Liu, G. X., C. Derst, G. Schlichthorl, S. Heinen, G. Seebohm, A. Bruggemann, W. Kummer, R. W. Veh, J. Daut, and R. Preisig-Muller. 2001. Comparison of cloned Kir2 channels with native inward rectifier K+ channels from guinea-pig cardiomyocytes. *J. Physiol.* 532:115–126.

Lopatin, A. N., and C. G. Nichols. 2001. Inward rectifiers in the heart: an update on I(K1). *J. Mol. Cell. Cardiol.* 33:625–638.

Lopes, C. M., H. Zhang, T. Rohacs, T. Jin, J. Yang, and D. E. Logothetis. 2002. Alterations in conserved Kir channel-PIP2 interactions underlie channelopathies. *Neuron.* 34:933–944.

Lowry, O. H., N. Rosenbrough, A. Farr, and R. Randall. 1951. Protein measurements with folin phelon reagent. *J. Biol. Chem.* 193:265–275.

Makhina, E. N., A. J. Kelly, A. N. Lopatin, R. W. Mercer, and C. G. Nichols. 1994. Cloning and expression of a novel human brain inward rectifier potassium channel. *J. Biol. Chem.* 269:20468–20474.

Markwell, M. A. K., S. M. Haas, L. L. Bieber, and N. E. Tolbert. 1978. A modification of the Lowry procedure to simplify protein determination in the membrane and lipoprotein samples. *Anal. Biochem.* 87:206–210.

Martens, J. R., R. Navarro-Polanco, E. A. Coppock, A. Nishiyama, L. Parshley, T. D. Grobaski, and M. M. Tamkun. 2000. Differential targeting of shaker-like potassium channels to lipid rafts. *J. Biol. Chem.* 275:7443–7446.

Martens, J. R., K. O'Connell, and M. Tamkun. 2004. Targeting of ion channels to membrane microdomains: localization of KV channels to lipid rafts. *Trends Biochem. Sci.* 25:16–21.

Martens, J. R., N. Sakamoto, S. A. Sullivan, T. D. Grobaski, and M. M. Tamkun. 2001. Isoform-specific localization of voltage-gated K+ channels to distinct lipid raft populations. Targeting of Kv1.5 to caveolae. *J. Biol. Chem.* 276:8409–8414.

McCloskey, H. M., G. H. Rothblat, and J. M. Glick. 1987. Incubation of acetylated low-density lipoprotein with cholesterol-rich dispersions enhances cholesterol uptake by macrophages. *Biochim. Biophys. Acta.* 921:320–332.

McLaughlin, S., J. Wang, A. Gambhir, and D. Murray. 2002. PIP(2) and proteins: interactions, organization, and information flow. *Annu. Rev. Biophys. Biomol. Struct.* 31:151–175.

Melnyk, P., L. Zhang, A. Shrier, and S. Nattel. 2002. Differential distribution of Kir2.1 and Kir2.3 subunits in canine atrium and ventricle. *Am. J. Physiol. Heart Circ. Physiol.* 283:H1123–H1133.

Miake, J., E. Marban, and H. B. Nuss. 2003. Functional role of inward rectifier current in heart probed by Kir2.1 overexpression and dominant-negative suppression. *J. Clin. Invest.* 111:1529–1536.

Munro, S. 2003. Lipid rafts: elusive or illusive? *Cell.* 115:377–388.

Neusch, C., J. H. Weishaupt, and M. Bahr. 2003. Kir channels in the CNS: emerging new roles and implications for neurological diseases. *Cell Tissue Res.* 311:131–138.

Nolop, K. B., and U. S. Ryan. 1990. Enhancement of tumor necrosis factor-induced endothelial cell injury by cycloheximide. *Am. J. Physiol.* 259:L123–L129.

Perier, F., C. M. Radeke, and C. A. Vandenberg. 1994. Primary structure and characterization of a small-conductance inwardly rectifying potassium channel from human hippocampus. *Proc. Natl. Acad. Sci. USA.* 91:6240–6244.

Plaster, N. M., R. Tawil, M. Tristani-Firouzi, S. Canun, S. Bendahhou, A. Tsunoda, M. R. Donaldson, S. T. Iannaccone, E. Brunt, R. Barohn, J. Clark, F. Deymeer, A. L. George, Jr., F. A. Fish, A. Hahn, A. Nitu, C. Ozdemir, P. Serdaroglu, S. H. Subramony, G. Wolfe, Y. H. Fu, and L. J. Ptacek. 2001. Mutations in Kir2.1 cause the developmental and episodic electrical phenotypes of Andersen's syndrome. *Cell.* 105:511–519.

Polunovsky, V. A., C. H. Wendt, D. H. Ingbar, M. S. Peterson, and P. B. Bitterman. 1994. Induction of endothelial cell apoptosis by TNF alpha: modulation by inhibitors of protein synthesis. *Exp. Cell Res.* 214:584–594.

Preisig-Muller, R., G. Schlichthorl, T. Goerge, S. Heinen, A. Bruggemann, S. Rajan, C. Derst, R. W. Veh, and J. Daut. 2002. Heteromerization of Kir2.x potassium channels contributes to the phenotype of Andersen's syndrome. *Proc. Natl. Acad. Sci. USA.* 99:7774–7779.

Pruss, H., M. Wenzel, D. Eulitz, A. Thomzig, A. Karschin, and R. W. Veh. 2003. Kir2 potassium channels in rat striatum are strategically localized to control basal ganglia function. *Brain Res. Mol. Brain Res.* 110:203–219.

Raab-Graham, K. F., and C. A. Vandenberg. 1998. Tetrameric subunit structure of the native brain inwardly rectifying potassium channel Kir 2.2. *J. Biol. Chem.* 273:19699–19707.

Ren, Y. J., X. H. Xu, C. B. Zhong, N. Feng, and X. L. Wang. 2001. Hypercholesterolemia alters vascular functions and gene expression of potassium channels in rat aortic smooth muscle cells. *Acta Pharmacol. Sin.* 22:274–278.

Rohacs, T., J. Chen, G. D. Prestwich, and D. E. Logothetis. 1999. Distinct specificities of inwardly rectifying K^+ channels for phosphoinositides. *J. Biol. Chem.* 274:36065–36072.

Romanenko, V. G., G. H. Rothblat, and I. Levitan. 2002. Modulation of endothelial inward rectifier K^+ current by optical isomers of cholesterol. *Biophys. J.* 83:3211–3222.

Sampson, L. J., M. L. Leyland, and C. Dart. 2003. Direct interaction between the actin-binding protein filamin-A and the inwardly rectifying potassium channel, Kir2.1. *J. Biol. Chem.* 278:41988–41997.

Schram, G., P. Melnyk, M. Pourrier, Z. Wang, and S. Nattel. 2002. Kir2.4 and Kir2.1 K(+) channel subunits co-assemble: a potential new contributor to inward rectifier current heterogeneity. *J. Physiol.* 544: 337–349.

Schram, G., M. Pourrier, Z. Wang, M. White, and S. Nattel. 2003. Barium block of Kir2 and human cardiac inward rectifier currents: evidence for subunit-heteromeric contribution to native currents. *Cardiovasc. Res.* 59:328–338.

Shimano, H. 2001. Sterol regulatory element-binding proteins (SREBPs): transcriptional regulators of lipid synthetic genes. *Prog. Lipid Res.* 40: 439–452.

Shyng, S.-L., C. A. Cukras, J. Harwood, and C. G. Nichols. 2000. Structural determinants of PIP2 regulation of inward rectifier KATP channels. *J. Gen. Physiol.* 116:599–608.

Shyng, S. L., Q. Sha, T. Ferrigni, A. N. Lopatin, and C. G. Nichols. 1996. Depletion of intracellular polyamines relieves inward rectification of potassium channels. *Proc. Natl. Acad. Sci. USA.* 93:12014–12019.

Simons, K., and D. Toomre. 2000. Lipid rafts and signal transduction. *Nat. Rev. Mol. Cell Biol.* 1:31–39.

Soom, M., R. Schonherr, Y. Kubo, C. Kirsch, R. Klinger, and S. H. Heinemann. 2001. Multiple PIP2 binding sites in Kir2.1 inwardly rectifying potassium channels. *FEBS Lett.* 490:49–53.

Stockklausner, C., and N. Klocker. 2003. Surface expression of inward rectifier potassium channels is controlled by selective Golgi export. *J. Biol. Chem.* 278:17000–17005.

Takahashi, N., K. I. Morishige, A. Jahangir, M. Yamada, I. Findlay, H. Koyama, and Y. Kurachi. 1994. Molecular cloning and functional expression of cDNA encoding a second class of inward rectifier potassium channels in the mouse brain. *J. Biol. Chem.* 269:23274–23279.

Tillman, T. S., and M. Cascio. 2003. Effects of membrane lipids on ion channel structure and function. *Cell Biochem. Biophys.* 38:161–190.

Tong, Y., G. S. Brandt, M. Li, G. Shapovalov, E. Slimko, A. Karschin, D. A. Dougherty, and H. A. Lester. 2001. Tyrosine decaging leads to substantial membrane trafficking during modulation of an inward rectifier potassium channel. *J. Gen. Physiol.* 117:103–118.

Topert, C., F. Doring, E. Wischmeyer, C. Karschin, J. Brockhaus, K. Ballanyi, C. Derst, and A. Karschin. 1998. Kir2.4: a novel K+ inward rectifier channel associated with motoneurons of cranial nerve nuclei. *J. Neurosci.* 18:4096–4105.

Wang, Z., L. Yue, M. White, G. Pelletier, and S. Nattel. 1998. Differential distribution of inward rectifier potassium channel transcripts in human atrium versus ventricle. *Circulation.* 98:2422–2428.

Wischmeyer, E., F. Doring, and A. Karschin. 1998. Acute suppression of inwardly rectifying Kir2.1 channels by direct tyrosine kinase phosphorylation. *J. Biol. Chem.* 273:34063–34068.

Wischmeyer, E., and A. Karschin. 1996. Receptor stimulation causes slow inhibition of IRK1 inwardly rectifying K^+ channels by direct protein-kinase A phosphorylation. *Proc. Natl. Acad. Sci. USA.* 93:5819–5823.

Yang, D., D. K. MacCallum, S. A. Ernst, and B. A. Hughes. 2003. Expression of the inwardly rectifying K+ channel Kir2.1 in native bovine corneal endothelial cells. *Invest. Ophthalmol. Vis. Sci.* 44:3511–3519.

Yeagle, P. L. 1991. Modulation of membrane function by cholesterol. *Biochimie.* 73:1303–1310.

Yin, H. L., and P. A. Janmey. 2003. Phosphoinositide regulation of the actin cytoskeleton. *Annu. Rev. Physiol.* 65:761–789.

Zaritsky, J. J., D. M. Eckman, G. C. Wellman, M. T. Nelson, and T. L. Schwarz. 2000. Targeted disruption of Kir2.1 and Kir2.2 genes reveals the essential role of the inwardly rectifying K^+ current in K^+-mediated vasodilation. *Circ. Res.* 87:160–166.

Zhang, H., C. He, X. Yan, T. Mirshahi, and D. E. Logothetis. 1999. Activation of inwardly rectifying K+ channels by distinct Ptdlns(4,5)P2 interactions. *Nat. Cell Biol.* 1:183–188.

Zhu, G., Z. Qu, N. Cui, and C. Jiang. 1999. Suppression of Kir2.3 activity by Protein Kinase C phosphorylation of the channel protein at threonine 53. *J. Biol. Chem.* 274:11643–11646.

Zobel, C., H. C. Cho, T. T. Nguyen, R. Pekhletski, R. J. Diaz, G. J. Wilson, and P. H. Backx. 2003. Molecular dissection of the inward rectifier potassium current (IK1) in rabbit cardiomyocytes: evidence for heteromeric co-assembly of Kir2.1 and Kir2.2. *J. Physiol.* 550:365–372.